Improved piezoelectric and energy harvesting characteristics in lead-free Fe$_2$O$_3$ modified KNN ceramics

**Indrani Coondoo · Neeraj Panwar · Hiroshi Maiwa ·
Andrei L. Kholkin**

Abstract Lead-free piezoelectric ceramics gained an increased attention due to their high piezoelectric properties combined with the absence of lead and other potentially hazardous elements. In this work, we used a unimorph cantilever beam arrangement to study piezoelectric energy harvesting in pristine K$_{0.5}$Na$_{0.5}$NbO$_3$ (KNN) and Fe$_2$O$_3$ modified KNN (KNFN) ceramics that are potential candidates for PZT replacement. The piezoelectric ceramics were synthesized using conventional solid state reaction method. The KNFN ceramics exhibited a superior piezoelectric performance: d_{33}=100 pC/N and mechanical quality factor (Q_m=135) as compared to KNN (d_{33}=83 pC/N; Q_m=76). In addition, the planar electromechanical coupling factor k_p was higher in case of KNFN having a value of 0.39 as compared to 0.34 for KNN. The KNFN harvester generated an output power of 0.38 mW/cm^3 at a load resistance of 470 kΩ for a transverse displacement amplitude of 1.2 mm. The prospects of using lead-free ceramics for piezoelectric energy harvesting are discussed.

I. Coondoo (✉) · A. L. Kholkin
Department of Materials and Ceramic Engineering & CICECO, University of Aveiro, Aveiro, Portugal
e-mail: indrani.coondoo@ua.pt

N. Panwar
Department of Physics, Central University of Rajasthan, Kishangarh, India

H. Maiwa
Materials and Human Environmental Sciences, Shonan Institute of Technology, Fujisawa, Japan

1 Introduction

With the advent of low-power and lightweight electronic devices, highly efficient power generation approaches are demanded. The energy requirements of these low and self-powered electronics cannot solely rely on the conventional batteries, where size, weight, safety or lifetime constraints are of major concern. This paved way for research in energy scavenging technologies which has received much global attention recently.

Energy harvesting is the process of converting available ambient energy into usable electrical energy via a transduction mechanism. Several conversion mechanisms that can be used to harvest energy are available: photovoltaic coupling, thermoelectric coupling and electromechanical coupling. Among the various available techniques, vibration energy harvesting is the most flexible method being developed. The vibration harvesters use one of the following three methods: electromagnetic (inductive), electrostatic (capacitive) or piezoelectric. The simplicity of piezoelectric transduction and the relative ease of implementation of piezoelectric systems into a wide variety of applications as compared to electrostatic or electromagnetic methods, makes it the foremost choice. The working principle is simple, wherein placing the piezoelectric device in a vibration rich environment (input vibration), the electromechanical coupling exhibited by piezoelectric materials causes mechanical strain or stress to develop in the device which is converted to electrical charge via piezoelectric effect. The most common piezoelectric energy harvesting configuration is the cantilever beam arrangement as shown in Fig. 1a. It consists of a cantilever that is made up of an upper piezoelectric element sandwiched between a pair of metal electrodes and a lower non-piezoelectric (passive) part. When the base of the system is subjected to vibrations, the input force causes a mechanical stress on piezoelectric material. As a consequence, an electric charge is induced owing to the piezoelectric effect

Fig. 1 Schematic of a **a** typical cantilever beam arrangement and **b** measurement set-up for piezoelectric energy harvesting
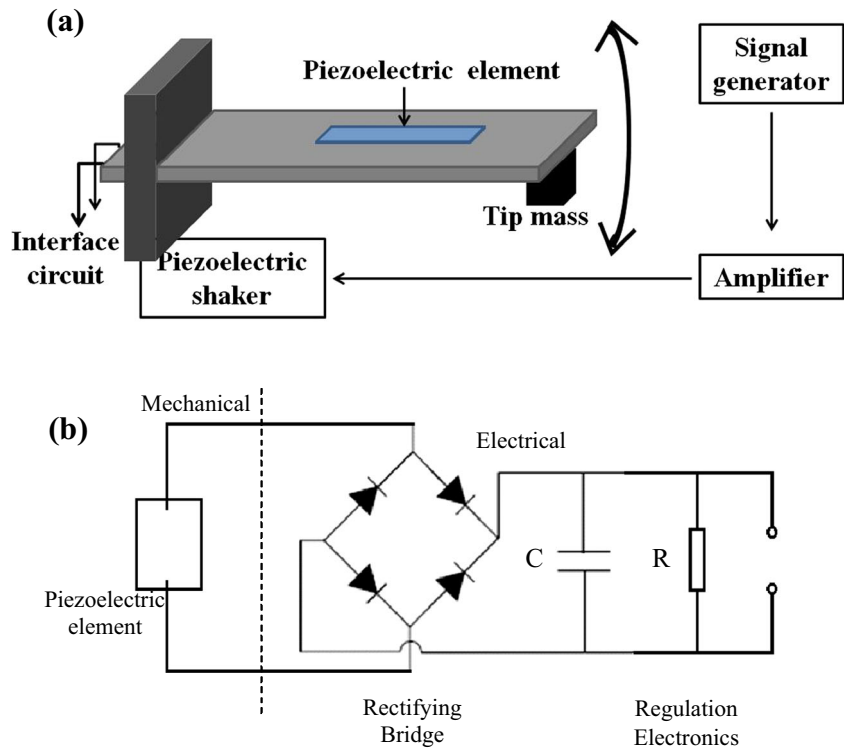
whose magnitude is proportional to the mechanical stress. Optimal performance of the harvesting system is obtained when the frequency of ambient vibration closely matches the resonant frequency of the harvester beam. The current piezoelectric harvesting technologies can harvest electrical power in the level of μW-mW, usually at a specific resonance frequency [1–3]. This low power output necessitates not only the design of ultra-low power logic circuits but also the efficient power delivery interface circuits that can extract the maximum power available out of the energy harvesters. Figure 1b portrays the schematic diagram of the measurement set-up. In general, the power generated from vibration to electrical energy conversion can be approximated at the resonance frequency of the system by Eq. 1 [4]:

$$P = \frac{mY_o^2\omega_n^3}{4\varsigma},\qquad\text{(Eq.1)}$$

where $\omega_n = \sqrt{k/m}$ is the system resonant frequency, m is the proof mass, k, is the spring constant, Y_o is the amplitude of vibration and ς is the total damping ratio (electrical and mechanical $\varsigma = c/2m\omega_n$), where c is the damping coefficient. Equation 1 signifies that power is inversely proportional to the damping ratio which should be minimized through proper selection of materials and design. Thus, keeping all the factors constant, the power of energy harvester can be enhanced by selecting a piezoelectric material with higher quality factor. Also, since P is directly proportional to proof mass of the

system, therefore reducing the size of harvester reduces the conversion efficiency. The metal mass on the tip of the cantilever is used to decrease the structure's natural frequency for application under low-frequency vibrations (most frequently used for energy harvesting). The efficiency of converting mechanical energy into electrical energy (η) has been evaluated using Q_m and k_p values [5]. It is given by Eq. 2:

$$\eta = \frac{k^2}{2(1-k^2)} \bigg/ \left(\frac{1}{Q_m} + \frac{k^2}{2(1-k^2)} \right)\qquad\text{(Eq.2)}$$

where k is the electromechanical coupling factor and Q_m is the quality factor. Therefore, the selection of proper piezoelectric materials and piezoelectric transducer configuration are key factors for their implementation in useful technology [6–10]. Fundamentally, to minimize degradation of the output power from a piezoelectric energy harvester, not only the quality factor but the coupling coefficient should be maximized by choosing the largest piezoelectric strain coefficient d and the smallest dielectric constant ε ($k \propto \frac{d}{\sqrt{\varepsilon}}$).

There are numerous reports in the literature on the bulk and thin film based piezoelectric harvesting devices. Umeda et al. [11] were among the pioneers to fabricate and to study a PZT-based generator and proposed an electrical equivalent model describing a transformation of the mechanical impact energy into electrical energy stimulated by an impact with a steel ball.

Jeon et al. [12] obtained an output power of 1.01 μW across a 5.2 MΩ load at the resonance frequency of 13.9 kHz. They used piezoelectric cantilevers having dimensions of $100 \times 60 \times 0.48$ μm^3 with inter-digitated electrodes. Sufficiently high harvesting energy density was demonstrated by Uppal et al. in the system Pb(Zr$_{0.52}$Ti$_{0.48}$)O$_3$-Pb(Zn$_{1/3}$Nb$_{2/3}$) (80.84 mJ/cm^3) [13]. Simulation conducted on a PZT film based energy harvesting structure showed that a power density of 80 μW/cm^3 at the operating frequency of 800 Hz could be obtained [14]. Beeby et al. reviewed the potential of piezoelectric energy harvesting and reported that power density of piezoelectric micro energy harvesting devices ranges between 10 and 40 μW/cm^3 in the acceleration and frequency range of 2.3–78.4 m/s^2 of 0.08–1 kHz, respectively [15]. For a curved-shape PZT unimorph, a power output of 250mW with RMS voltage of 1.8 V across a 10 Ω resistor at 2 Hz frequency was reported [16]. A modified vibration energy harvesting device based on rectangular cymbal transducer composed of 0.71PbMg$_{1/3}$Nb$_{2/3}$O$_3$- 0.29PbTiO$_3$ single crystal generated a high peak voltage of 45.7 V and maximum power of 14 mW at 500 Hz under a cyclic force of 0.55 N peak value [17]. Recently, Choi et al. obtained a high output energy density of 231 mW/cm^3 for the harvester fabricated using 0.69Pb(Zr$_{0.47}$Ti$_{0.53}$)O$_3$-0.31Pb[(Zn$_{0.4}$Ni$_{0.6}$)$_{1/3}$Nb$_{2/3}$]O$_3$) [18]. Halim et al. obtained 377 μW peak power at 14.5 Hz under 0.6 g acceleration with corresponding power density 58.8 μWcm^{-3} in PMN-PT single crystals [19]. Recently, nanogenerator based on PZT aligned nanofibers has been reported with an output voltage peak of 1.63 V and a power of 0.03 μW [20]. As one of the first examples of environmental concern, BaTiO$_3$ nanogenerator was fabricated on a plastic substrate and showed an output voltage up to 1.0 V and a power density of 7 mW/cm^3 [21].

Previous work has been mainly conducted on Pb-based ceramics and single crystals. However, environmental concerns and possible ban of using lead [22] have stimulated research on lead free alternatives, in particular, (Na$_{0.5}$K$_{0.5}$)NbO$_3$ (KNN)-based ceramics because of their relatively high piezoelectric properties and elevated Curie temperatures [23]. However, not much work has been done in this direction so far. In the present report energy harvesters based on pure KNN and 0.25 mol% Fe$_2$O$_3$-added KNN (KNFN) ceramics were fabricated and their harvesting performance was evaluated aiming at their potential use in energy harvesting applications.

2 Experimental

The following lead-free piezoelectric compositions were synthesized using the conventional solid state reaction method:

K$_{0.5}$Na$_{0.5}$NbO$_3$(KNN)
K$_{0.5}$Na$_{0.5}$NbO$_3$ + 0.25 mol% Fe$_2$O$_3$(KNFN)
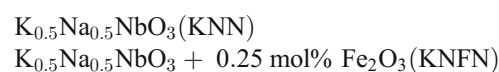
Stoichiometric ratio of the metal oxides and carbonates (Sigma-Aldrich): Na$_2$CO$_3$ (99.8%), K$_2$CO$_3$ (99.9%), CaCO$_3$ (99.9%), Nb$_2$O$_5$ (99.95%) and Fe$_2$O$_3$ (99.0%) were mixed thoroughly and calcined at 875 °C for 4 h. The calcined powders were pressed at 300 MPa and sintered at 1090 °C (KNN) and 975 °C (KNFN) for 2 h in air. The crystalline structure of the sintered samples was examined using x-ray diffraction (XRD) technique. The microstructure was observed using a field emission scanning electron microscope (Hitachi S4100).

The piezo-elements in the shape of square parallelopiped were polished to a dimension: $4 \times 6 \times 0.4$ mm^3 and thereafter adhered to the Fibre-reinforced plastic (FRP) beam (105mm× 10mm×1.6mm). The unimorph structure having a natural frequency of 57 Hz was oscillated by a vibration generator. The displacements of the unimorph were monitored with an acceleration meter attached to the other end. The voltages across the load resistor were measured by oscilloscope.

3 Results and discussion

Figure 2a shows the XRD patterns of KNN and KNFN ceramics. Both compositions demonstrate an orthorhombic structure without any detectable secondary phases. It may therefore be assumed that Fe^{3+} ions in the KNFN ceramic are incorporated into the matrix of the KNN phase. Owing to their similar sizes, the Fe^{3+} ions (0.69 Å) enter Nb^{5+} (0.68 Å) sites and act as an acceptor dopant. Oxygen vacancies will be introduced into the lattice to compensate for the charge imbalance with the doping of acceptor Fe. When one Fe^{3+} replaces one Nb^{5+}, an oxygen vacancy is created to maintain the charge neutrality. This can be expressed using the Krger-Vink notation as follows:

$$Fe_2O_3 \rightarrow Fe_{Nb}'' + V_o^{\bullet\bullet} \qquad \text{(Eq.3)}$$
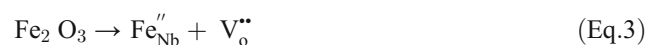
where Fe$_{Nb}''$ and V$_o^{\bullet\bullet}$ epresent Fe occupying the Nb site and an effectively doubly positive charged oxygen vacancy, respectively.

The microstructures of the KNN and KNFN ceramics were observed by FESEM. Figure 2b presents the surface FESEM images of the samples having characteristic quadratic grains. KNFN had a high relative density of 94% having a dense microstructure with a few larger grains (~9 μm). The generated oxygen vacancies in KNFN accelerate the mass transport process and improves the grain growth. Thus, KNFN is expected to exhibit lower dielectric losses than that of the KNN ceramics because of the lower grain boundary area which acts as defects. Table 1 enlists various dielectric and piezoelectric parameters of the respective compositions. It is observed that dielectric constant is higher for KNN (650) as compared to KNFN (430). Whereas the quality factor (Q_m), piezoelectric

Fig. 2 a XRD patterns and **b** SEM images of KNN and KNFN ceramics
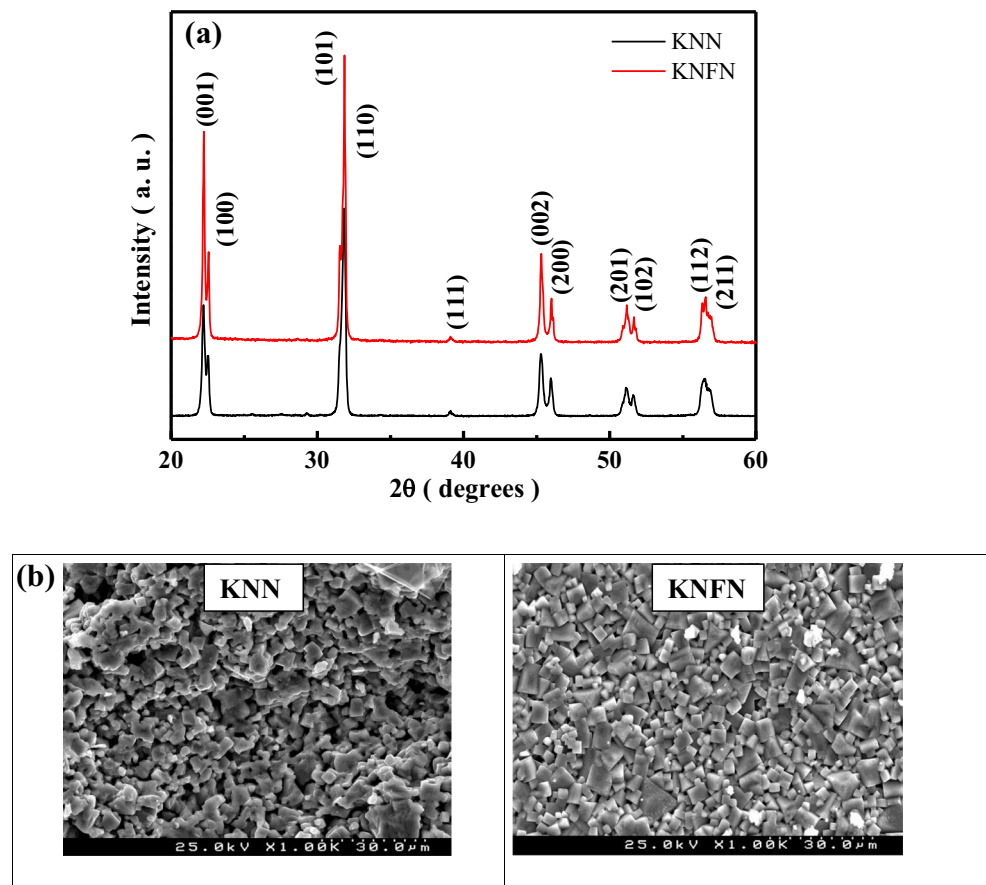
charge coefficient (d_{33}) and planar electromechanical coupling factor (k_p) are higher for KNFN. In addition, KNFN ceramic is expected to have a higher Q_m than KNN, because of the hardening effect of the acceptor Fe^{3+} ions. The introduced oxygen vacancies act as pinning points for the domain walls causing a reduced domain wall motion, thereby increasing Q_m [24, 25]. Since piezoelectric coupling coefficient k is proportional to piezoelectric constant and inversely to dielectric constant (as discussed in the introduction section), hence a higher k is observed for KNFN. The efficiency of the harvesters, fabricated in this work was calculated using Q_m and k_p values in Eq. 2 [18] and was estimated to be around 83% and 92% for KNN and KNFN, respectively. Based on these

parameters, the KNFN composition is expected to exhibit better harvesting characteristics as compared to pure KNN.

Figure 3 represents the output voltage and power of the KNN harvester measured at various frequencies and load resistances. Figure 3a depicts the frequency dependence of the output voltage generated by KNN over a frequency range of 40–70 Hz. The energy harvester was subjected to a constant base acceleration to measure voltage generated across the load resistor. The output voltage increases gradually as the operating frequency increases up to the resonant frequency and thereafter drops off when the exciting frequency exceeds the resonant frequency (57 Hz for KNN). The resonant frequency of a vibration energy harvester is one of the most important design parameters, because the maximum output power can be obtained when the vibration frequency matches the resonant frequency. It is well-known that the power output will be dramatically reduced when the driving vibration frequency deviates from the resonant frequency of the device [4]. It was also noted that the resonance frequency values for both the compositions were similar, because of the similar size of the harvesters [18]. The peak-to-peak voltage (V_p) of the generating beam versus load resistance under various displacements is shown in Fig. 3b. As expected, it is observed that the generating beam's output voltage increases with increasing resistive load and displacement. The output voltage at 10

Table 1 Dielectric and Piezoelectric properties

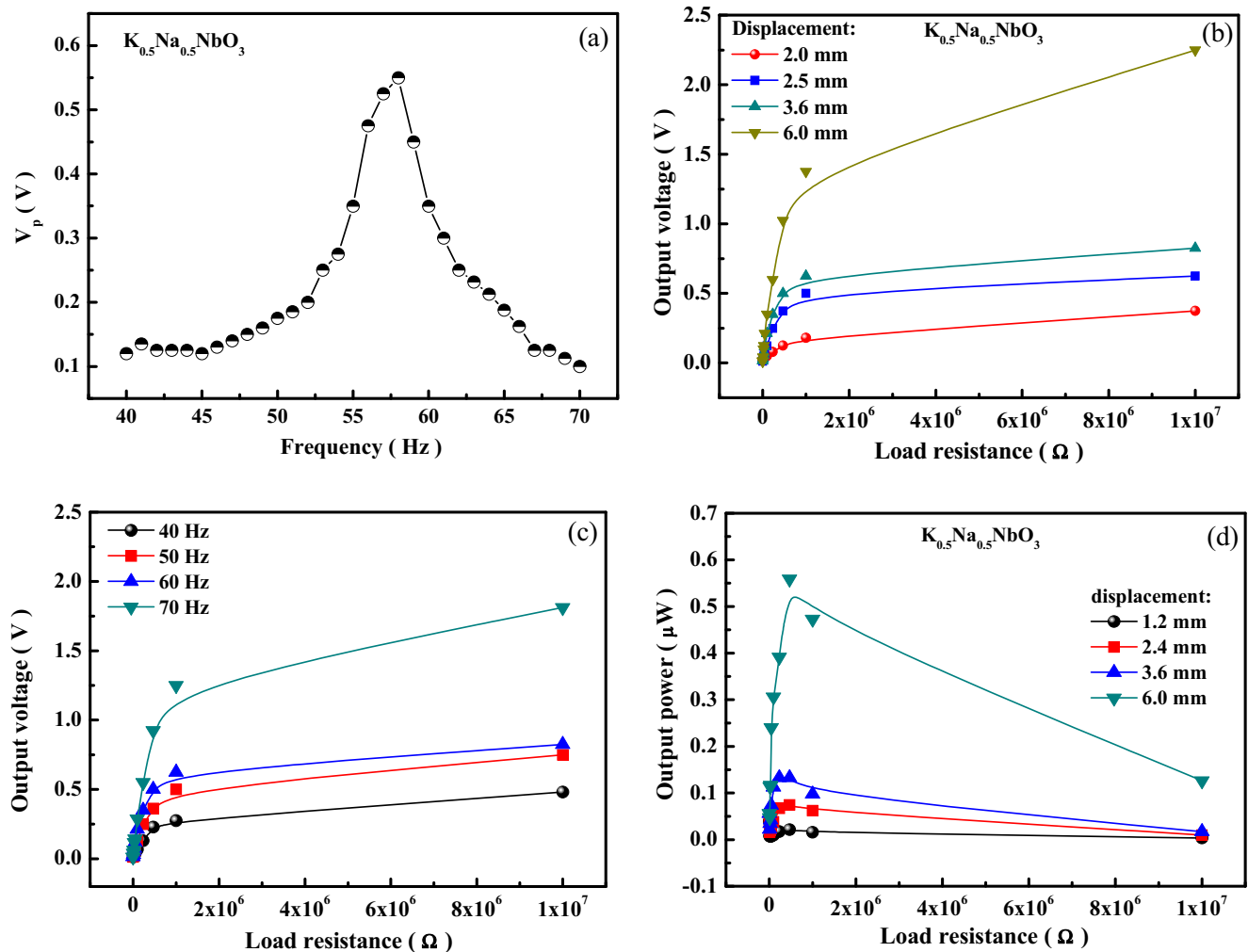| Properties	KNN	KNFN
ρ (g/cm³)	4.19	4.39
ε_r	650	430
Q_m	76	135
d_{33} (pC/N)	83	100
g_{33} (10^{-3} Vm/N)	14	26
$d_{33}.g_{33}$ (m²/N)	1162	2600
k_p	0.34	0.39

Fig. 3 **a** Frequency response of output voltage **b** Output voltage as a function of load resistance at different displacements at 60 Hz **c** Output voltage as a function of load resistance for different frequencies at a displacement of 3.6 mm and **d** Output power measured at various load resistances of the KNN energy harvester at 60 Hz and various displacements

MΩ load resistance increased from ~0.38 V for a 2 mm displacement to ~2.25 V for a displacement of 6 mm. Figure 3c represents the variation of the output voltage at various frequencies for a fixed base acceleration. The output voltage value increased with an increase in frequency value from 40 to 70 Hz. It is found that higher operating frequency results in higher voltage. The optimal load for maximum power transfer was determined by varying the load resistance values under various displacement deformation as shown in Fig. 3d. In general, there are two ways to determine electric power from piezoelectric unimorph ceramic harvester. Electric power available from periodic excitation of the piezoelectric unimorph is given as [26]:

$$P_e = 2 \times E_c \times f \qquad (\text{Eq.4})$$

where E_c $\left(E_c \left(= \frac{1}{2} C_p V_p^2\right)\right)$ is the energy stored in a capacitor, C_p is the equivalent source capacitance, V_p is the voltage at full

compression and f is the operating frequency. Alternatively, the power, P, generated from a stand-alone piezoelectric harvesting device irrespective of its geometry (cantilever, membrane, etc.) can be written as [27]:

$$P = \frac{V_o^2 R_L}{(R_S + R_L)^2} \qquad (\text{Eq.5})$$

where V_o is the open voltage generated from the piezoelectric beam. When the applied external resistive load at which the output power is harvested is equal to the source resistance/ impedance R_S condition referred to as impedance matching), maximum piezoelectric power output is obtained [28]. Thus, the maximum output power P_{max} is given as:

$$P_{max} = \frac{V_o^2}{4R_S} \qquad (\text{Eq.6})$$

Experimentally, the piezoelectric power output is equal to $V_L^2/4R_L$ where V_L is the measured peak-peak voltage across the load resistance R_L. Further analysis shows that V_o and the corresponding power output from the piezoelectric mechanism is inversely proportional to ε (the dielectric constant of the piezoelectric material) and directly related to d_{3i} (d_{3i} is the piezoelectric strain constant, where i is either 1 or 3 depending on whether the piezoelectric mode is d_{31} or d_{33}). Also, since mechanical input power employed on the unimorph, $P_m = F \times d \times f$, the larger the displacement d of piezoelectric unimorph ceramic, the greater electric power is obtained. As observed for KNN harvester (Fig. 3d), a maximum power of 0.02 μW was transferred to a 470 kΩ resistor for a transverse displacement amplitude 1.2 mm which increased up to 0.56 μW for 6 mm displacement.

Figure 4a and b compares the obtained peak output voltage and power delivered by KNN and KNFN at the optimal load under a fixed base acceleration (transverse displacement: 2.4 mm). The output voltage is observed to increase with load resistance. It is confirmed that the power generated from KNFN is much higher than that for pure KNN which could be a result of the large d_{33} and d_{31} values of the former. A peak power of 3.67 μW is generated at 470 kΩ for KNFN as compared to pure KNN (0.089 μW). The value obtained for KNFN is higher than that obtained in textured 0.945 $(Bi_{0.5}Na_{0.5})$ TiO_3–$0.55BaTiO_3$ (BNTBT) ceramics containing $SrTiO_3$ (STO) templates [29]. The output power in our case is also higher than that for thick film bimorph PZT harvester [30], and that reported for KNN (1.1 μW) and PZT (1.0 μW) thin-films [31] and 1.6 μW for KNN in [32]. However, it is lower than that reported for CuO-added $(K_{0.5}Na_{0.5})$ NbO_3 [33]. Figure 4c shows the power densities for the studied compositions as a function of the load resistance. A peak power density value of 0.38 mW/cm^3 is observed for KNFN. Since KNFN had a higher k_p value, which influences the energy transformation efficiency, it is also responsible for the improvement of the output power of the KNFN harvester. Addition of iron oxide in KNN, not only improved piezoelectric coefficients but also enhanced the Q_m. Quality factor is inversely proportional to the damping in an oscillating system
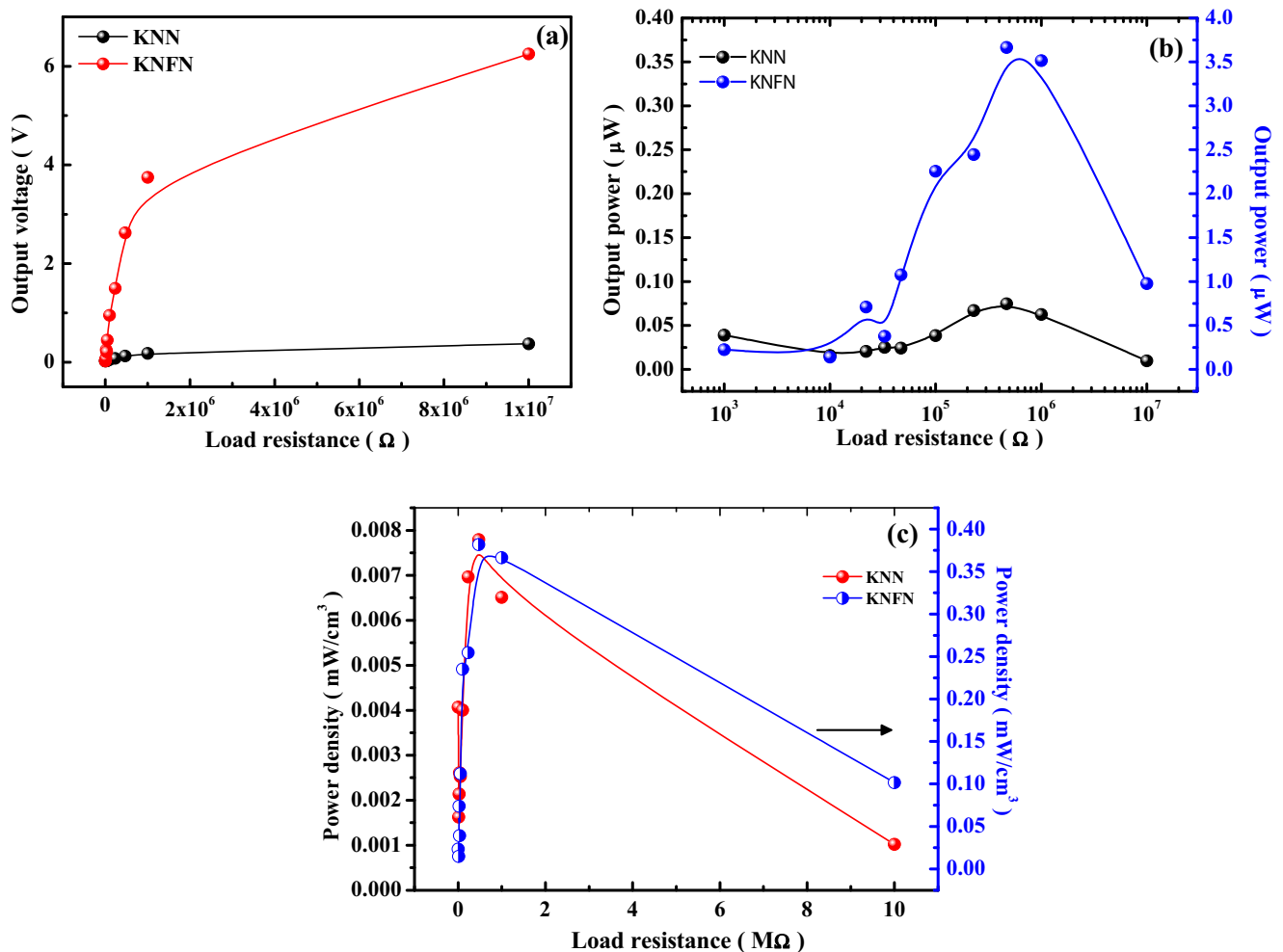

Fig. 4 A comparison of **a** Output voltage at a displacement of 1 mm **b** output power and **c** power density as a function of load resistance for the KNN and KNFN energy harvesters at a displacement of 2 mm

caused by energy loss via heat transfer and therefore is an important design issue in order to optimize the power harvesting ability. A system with a high Q_m value, does not dissipate much energy to heat, thereby making more energy available for harvesting through a piezoelectric device. Therefore, it may be concluded that adding Fe_2O_3 in KNN is effective in enhancing the properties suitable for vibration energy harvesting application.

4 Conclusions

Single phase KNN and KNFN ceramics were synthesized by the conventional solid state reaction method. The KNFN ceramics have higher piezoelectric charge coefficient values and smaller permittivity as compared to the KNN ceramic. Moreover, the Q_m value almost doubled with the addition of Fe_2O_3 in KNN. This resulted in higher power output in KNFN composition. The KNFN harvester fabricated in the present case, generated a high output power of 3.67 μW as compared to 0.089 μW for KNN at a load resistance of 470 kΩ. The efficiency for the harvesters fabricated in this work was estimated as 83% and 92% using the k_p and Q_m values for KNN and KNFN, respectively. Hence Fe_2O_3 serves as an effective sintering aid that not only reduces the synthesis temperature but also improves the harvesting capabilities than pure KNN. Therefore, KNFN ceramics are considered as potential candidate materials for piezoelectric energy harvesting application.

References

1. S. Anton, H. Sodano, Smart Mater. Struct. **16**, R1 (2007)
2. Y. Hu, F.Y. Zhang, C. Xu, L. Ling, R.L. Snyder, Z.L. Wang, Nano Lett. **11**, 2572 (2011)
3. A. Erturk, J. Hoffmann, D.J. Inman, Appl. Phys. Lett. **94**, 9254102 (2009)
4. S. Priya, J. Electroceram. **19**, 165 (2007)
5. C.D. Richards, M.J. Anderson, D.F. Bahr, R.F. Richards, J. Micromech. Microeng. **14**, 717 (2004)
6. H. Kim, V. Bedekar, R. Islam, W.H. Lee, D. Leo, S. Priya, IEEE Ultrason. Freq. Ferroelectr. Control **55**, 1900 (2008)
7. I.T. Seo, Y.J. Cha, I.Y. Kang, J.H. Choi, S. Nahm, T.H. Seung, J.H. Paik, J. Am. Ceram. Soc. **94**, 3629 (2011)
8. R.A. Islam, S. Priya, Appl. Phys. Lett. **88**, 032903 (2006)
9. S. Priya, IEEE Trans. Ultrason. Ferroelectr. Freq. Control **57**, 2610 (2010)
10. S. Priya, J. Ryu, C.S. Park, J. Oliver, J.J. Choi, D.S. Park, Sensors **9**, 6362 (2009)
11. M. Umeda, K. Nakamura, S. Ueha, Jpn. J. Appl. Phys. **35**, 3267 (1996)
12. Y.B. Jeon, R. Sood, J.H. Jeong, S.G. Kim, Sensors Actuators A **122**, 16 (2005)
13. N. Uppal, P. Shikolas, S. Priya, Ferroelectr. Lett. **32**, 67 (2006)
14. E.K. Reilly, E. Carleton, P.K. Wright, *Proceedings: International workshop on wearable & implantable body sensor networks, BSN 2006* 38 (2006).
15. S.P. Beeby, M.J. Tudor, N.M. White, Meas. Sci. Technol. **17**, R175 (2006)
16. N.S. Shenck, J.A. Paradiso, IEEE Micro. **21**, 30 (2001)
17. B. Ren, S.W. Or, X. Zhao, H. Luo, J. Appl. Phys. **107**, 034501 (2010)
18. C.H. Choi, I.T. Seo, D. Song, M.S. Jang, B.Y. Kim, S. Nahm, T.H. Sung, H.C. Song, J. Euro. Ceram. Soc. **33**, 1343 (2013)
19. M.A. Halim, S. Khym, J.Y. Park, J. Appl. Phys. **114**, 044902 (2013)
20. X. Chen, S. Xu, N. Yao, Y. Shi, Nano Lett. **10**, 2133 (2010)
21. K.I. Park, S. Xu, Y. Liu, G.T. Hwang, S.J.L. Kang, Z.L. Wang, K.J. Lee, Nano Lett. **10**, 4939 (2010)
22. http://www.rohs.eu/english/index.html.
23. H.Y. Park, I.T. Seo, M.K. Choi, S. Nahm, H.G. Lee, H.W. Kang, B.H. Choi, J. Appl. Phys. **104**, 034103 (2008)
24. L. Wu, C.C. Wei, T.S. Wu, H.C. Liu, J. Phys. C Solid State Phys. **16**, 2813 (1983)
25. D. Lin, K.W. Kwok, H.L.W. Chan, J. Phys. D. Appl. Phys. **41**, 045401 (2008)
26. Y. Ting, G. Hariyanto, B.K. Hou, C.Y. Huang, *Proceedings of the IEEE International Conference on Information and Automation*, (China, June 22–25 2009), pp 778
27. V.R. Challa, M.G. Prasad, F.T. Fisher, Smart Mater. Struct. **18**, 095029 (2009)
28. E. Minazara, D. Vasic, F. Costa, G. Poulin, Ultrasonics **44**, 699 (2006)
29. S.J. Jeong, D.S. Lee, M.S. Kim, D.H. Im, I.S. Kim, K.H. Cho, Ceram. Int. **38S**, S369 (2012)
30. M. Colin, S. Basrour, L. Rufer, C. Bantignies, A. Nguyen-Dinh, J. Physics, Conf Ser **476**, 012133 (2013)
31. I. Kanno, H. Kotera, K. Shibata, F. Horikiri and T. Mishima, *Proceedings Power MEMS*, (2011), pp 110
32. Y. Tsujiura, E. Suwa, F. Kurokawa, H. Hida, K. Suenaga, K. Shibata, I. Kanno, Jpn. J. Appl. Phys. **52**, 09KD13 (2013)
33. I.T. Seo, C.H. Choi, D. Song, M.S. Jang, B.Y. Kim, S. Nahm, Y.S. Kim, T.H. Sung, H.C. Song, J. Am. Ceram. Soc. **96**, 1024 (2013)